Supporting information

Additional Supporting Information may be found in the online version of this article:

Table S1. Primers used for nucleotide sequence analysis of TXA_2R.

Please note: Wiley-Blackwell are not responsible for the content or functionality of any supporting materials supplied by the authors. Any queries (other than missing material) should be directed to the corresponding author for the article.

References

1 Davì G, Patrono C. Platelet activation and atherothrombosis. *N Engl J Med* 2007; **357**: 2482–94.

2 Tomiyama Y, Shiraga M, Shattil SJ. Platelet membrane proteins as adhesion receptors. In: Gresele P, Page C, Fuster V, Vermylen J, eds. *Platelets in Thrombotic and Non-thrombotic Disorders: Pathophysiology, Pharmacology and Therapeutics*. Cambridge, UK: Cambridge University Press, 2002: 80–92.

3 Antiplatelet Trialists' Collaboration. Collaborative overview of randomised trials of antiplatelet therapy prevention of death, myocardial infarction, and stroke by prolonged antiplatelet therapy in various categories of patients. *BMJ* 1994; **308**: 81–106.

4 Antithrombotic Trialists' Collaboration. Collaborative meta-analysis of randomised trials of antiplatelet therapy for prevention of death, myocardial infarction, and stroke in high risk patients. *BMJ* 2002; **324**: 71–86.

5 CAPRIE Steering Committee. A randomised, blinded, trial of clopidogrel versus aspirin in patients at risk of ischaemic events (CAPRIE). *Lancet* 1996; **346**: 1329–39.

6 Cattaneo M, Zighetti ML, Lombardi R, Martinez C, Lecchi A, Conley PB, Ware J, Ruggeri ZM. Molecular bases of defective signal transduction in the platelet $P2Y_{12}$ receptor of a patient with congenital bleeding. *Proc Natl Acad Sci USA* 2003; **100**: 1978–83.

7 Nurden P, Nurden AT. Congenital disorders associated with platelet dysfunctions. *Thromb Haemost* 2008; **99**: 253–63.

8 Hirata M, Hayashi Y, Ushikubi F, Yokota Y, Kageyama R, Nakanishi S, Narumiya S. Cloning and expression of cDNA for a human thromboxane A_2 receptor. *Nature* 1991; **349**: 617–20.

9 Habib A, FitzGerald GA, Maclouf J. Phosphorylation of the thromboxane receptor α, the predominant isoform expressed in human platelets. *J Biol Chem* 1999; **274**: 2645–51.

10 Nakahata N. Thromboxane A_2: physiology/pathophysiology, cellular signal transduction and pharmacology. *Pharmacol Ther* 2008; **118**: 18–35.

11 Hirata T, Kakizuka A, Ushikubi F, Fuse I, Okuma M, Narumiya S. Arg60 to Leu mutation of the human thromboxane A_2 receptor in a dominantly inherited bleeding disorder. *J Clin Invest* 1994; **94**: 1662–7.

12 Higuchi W, Fuse I, Hattori A, Aizawa Y. Mutations of the platelet thromboxane A_2 (TXA_2) receptor in patients characterized by the absence of TXA_2-induced platelet aggregation despite normal TXA_2 binding activity. *Thromb Haemost* 1999; **82**: 1528–31.

13 Mumford AD, Dawood BB, Daly ME, Murden SL, Williams MD, Protty MB, Spalton JC, Wheatley M, Mundell SJ, Watson SP. A novel thromboxane A_2 receptor D304N variant that abrogates ligand binding in a patient with a bleeding diathesis. *Blood* 2010; **115**: 363–9.

14 Kamae T, Shiraga M, Kashiwagi H, Kato H, Tadokoro S, Kurata Y, Tomiyama Y, Kanakura Y. Critical role of ADP interaction with P2Y12 receptor in the maintenance of αIIbβ3 activation: association with Rap1B activation. *J Thromb Haemost* 2006; **4**: 1379–87.

15 Kato H, Honda S, Yoshida H, Kashiwagi H, Shiraga M, Honma N, Kurata Y, Tomiyama Y. SHPS-1 negatively regulates integrin αIIbβ3 function through CD47 without disturbing FAK phosphorylation. *J Thromb Haemost* 2005; **3**: 763–74.

16 Honda S, Tomiyama Y, Shiraga M, Tadokoro S, Takamatsu J, Saito H, Kurata Y, Matsuzawa Y. A two-amino acid insertion in the Cys146- Cys167 loop of the α_{IIb} subunit is associated with a variant of Glanzmann thrombasthenia. Critical role of Asp163 in ligand binding. *J Clin Invest* 1998; **102**: 1183–92.

17 Shiraga M, Kamae T, Akiyama M, Tadokoro S, Kashiwagi H, Oritani K, Kurata Y, Tomiyama Y, Kanakura Y. $P2Y_{12}$-independ transient activation and $P2Y_{12}$-dependent prolonged activation of platelet Integrin αIIbβ3. *Blood* 2006; **108**: 435a.

18 Tadokoro S, Nakazawa T, Kamae T, Kiyomizu K, Kashiwagi H, Honda S, Kanakura Y, Tomiyama Y. A potential role for α-actinin in inside-out αIIbβ3 signaling. *Blood* 2011; **117**: 250–8.

19 Gurevich VV, Gurevich EV. GPCR monomers and oligomers: it takes all kinds. *Trends Neurosci* 2008; **31**: 74–81.

20 Laroche G, Lépine MC, Thériault C, Giguère P, Giguère V, Gallant MA, de Brum-Fernandes A, Parent JL. Oligomerization of the alpha and beta isoforms of the thromboxane A_2 receptor: relevance to receptor signaling and endocytosis. *Cell Signal* 2005; **17**: 1373–83.

21 Nieswandt B, Schulte V, Zywietz A, Gratacap MP, Offermanns S. Costimulation of Gi- and G12/G13-mediated signaling pathways induces integrin αIIbβ3 activation in platelets. *J Biol Chem* 2002; **277**: 39493–8.

blood

2011 117: 5479-5484
Prepublished online March 31, 2011;
doi:10.1182/blood-2010-12-323691

Heterozygous *ITGA2B* R995W mutation inducing constitutive activation of the αIIbβ3 receptor affects proplatelet formation and causes congenital macrothrombocytopenia

Shinji Kunishima, Hirokazu Kashiwagi, Makoto Otsu, Naoya Takayama, Koji Eto, Masafumi Onodera, Yuji Miyajima, Yasushi Takamatsu, Junji Suzumiya, Kousaku Matsubara, Yoshiaki Tomiyama and Hidehiko Saito

Blood (print ISSN 0006-4971, online ISSN 1528-0020), is published weekly by the American Society of Hematology, 2021 L St, NW, Suite 900, Washington DC 20036.

Brief report

Heterozygous *ITGA2B* R995W mutation inducing constitutive activation of the αIIbβ3 receptor affects proplatelet formation and causes congenital macrothrombocytopenia

Shinji Kunishima,[1] Hirokazu Kashiwagi,[2] Makoto Otsu,[3] Naoya Takayama,[3] Koji Eto,[3] Masafumi Onodera,[4] Yuji Miyajima,[5] Yasushi Takamatsu,[6] Junji Suzumiya,[7] Kousaku Matsubara,[8] Yoshiaki Tomiyama,[2,9] and Hidehiko Saito[10]

[1]Department of Advanced Diagnosis, Clinical Research Center, National Hospital Organization Nagoya Medical Center, Nagoya, Japan; [2]Department of Hematology and Oncology, Graduate School of Medicine, Osaka University, Osaka, Japan; [3]Division of Stem Cell Therapy, Center for Stem Cell and Regenerative Medicine, Institute of Medical Science, University of Tokyo, Tokyo, Japan; [4]Department of Genetics, National Research Institute for Child Health and Development, Tokyo, Japan; [5]Department of Pediatrics, Anjo Kosei Hospital, Anjo, Japan; [6]Department of Medical Oncology, Hematology and Infectious Disease, Fukuoka University, Fukuoka, Japan; [7]Shimane University Hospital Cancer Center, Shimane, Japan; [8]Department of Pediatrics, Nishi-Kobe Medical Center, Kobe, Japan; [9]Department of Blood Transfusion, Osaka University Hospital, Osaka, Japan; and [10]Nagoya Central Hospital, Nagoya, Japan

Congenital macrothrombocytopenia is a genetically heterogeneous group of rare disorders. αIIbβ3 has not been implicated in these conditions. We identified a novel, conserved heterozygous *ITGA2B* R995W mutation in 4 unrelated families. The surface expression of platelet αIIbβ3 was decreased to 50% to 70% of control. There was spontaneous PAC-1 and fibrinogen binding to resting platelets without CD62p expression. The activation state of αIIbβ3 in 293T cells was higher for αIIb-W995 than for β3-H723 but was weaker than for β3-N562. FAK was spontaneously phosphorylated in αIIb-W995/β3-transfected 293T cells. These results indicate that αIIb-W995/β3 has a constitutive, activated conformation but does not induce platelet activation. αIIb-W995/β3-transfected CHO cells developed membrane ruffling and abnormal cytoplasmic protrusions. The increased size and decreased number of proplatelet tips in αIIb-W995/β3-transduced mouse fetal liver-derived megakaryocytes indicate defective proplatelet formation. We propose that activating mutations in *ITGA2B* and *ITGB3* represent the etiology of a subset of congenital macrothrombocytopenias. (*Blood.* 2011;117(20):5479-5484)

Introduction

Congenital macrothrombocytopenia is a genetically heterogeneous group of rare disorders.[1-4] The most frequent forms include *MYH9* disorders and Bernard-Soulier syndrome. In approximately half of cases of congenital macrothrombocytopenia, the pathogenesis remains unknown; thus, a definite diagnosis is unavailable. Glanzmann thrombasthenia is the most common congenital platelet disorder caused by qualitative or quantitative abnormality of the integrin αIIbβ3, in which the platelet counts and morphology are normal.[5] However, *ITGA2B* R995Q mutation has been reported in a patient with Glanzmann thrombasthenia-like phenotype and macrothrombocytopenia.[6,7] Recently, heterozygous *ITGB3* mutations were found in patients with congenital macrothrombocytopenia.[8-10] We report here a novel, conserved heterozygous *ITGA2B* R995W mutation in 4 unrelated families.

Methods

Patients

Twenty-seven patients with congenital macrothrombocytopenia, in whom *MYH9* disorders, heterozygous and homozygous Bernard-Soulier syndrome, type 2B von Willebrand disease, and *TUBB1* mutations were excluded, underwent mutational analysis of *ITGA2B* and *ITGB3*. Fifty-five consecutive patients were prospectively analyzed for the surface expression of platelet αIIbβ3. Written informed consent was obtained from all patients or their parents in accordance with the Declaration of Helsinki. Institutional review boards of Nagoya Medical Center and each of the participating institutions/hospitals approved this study.

Genetic analysis

The entire coding sequence of exons and exon-intron boundaries of *ITGA2B* (supplemental Table 1, available on the *Blood* Web site; see the Supplemental Materials link at the top of the online article) and *ITGB3* was amplified by polymerase chain reaction and sequenced. The disease-associated *ITGA2B* haplotype was determined by cloning and sequencing the polymerase chain reaction products.

Platelet glycoprotein analysis

Flow cytometry and immunoblotting were performed as described previously.[11,12] The activation state of αIIbβ3 was evaluated by the binding of the ligand-mimetic antibody PAC-1 (BD Biosciences) and FITC-labeled fibrinogen.[13]

Cloning, mutagenesis, and retroviral transduction

ITGA2B and *ITGB3* sequences were amplified from the patient's platelet cDNA and cloned into pcDNA3.1 (Invitrogen). T562N[13] and D723H[8] were introduced into *ITGB3* cDNA using site-directed mutagenesis. *ITGA2B* and *ITGB3* expression plasmids were cotransfected into 293T and CHO cells.

Submitted December 7, 2010; accepted March 18, 2011. Prepublished online as *Blood* First Edition paper, March 31, 2011; DOI 10.1182/blood-2010-12-323691.

The online version of this article contains a data supplement.

The publication costs of this article were defrayed in part by page charge payment. Therefore, and solely to indicate this fact, this article is hereby marked "advertisement" in accordance with 18 USC section 1734.

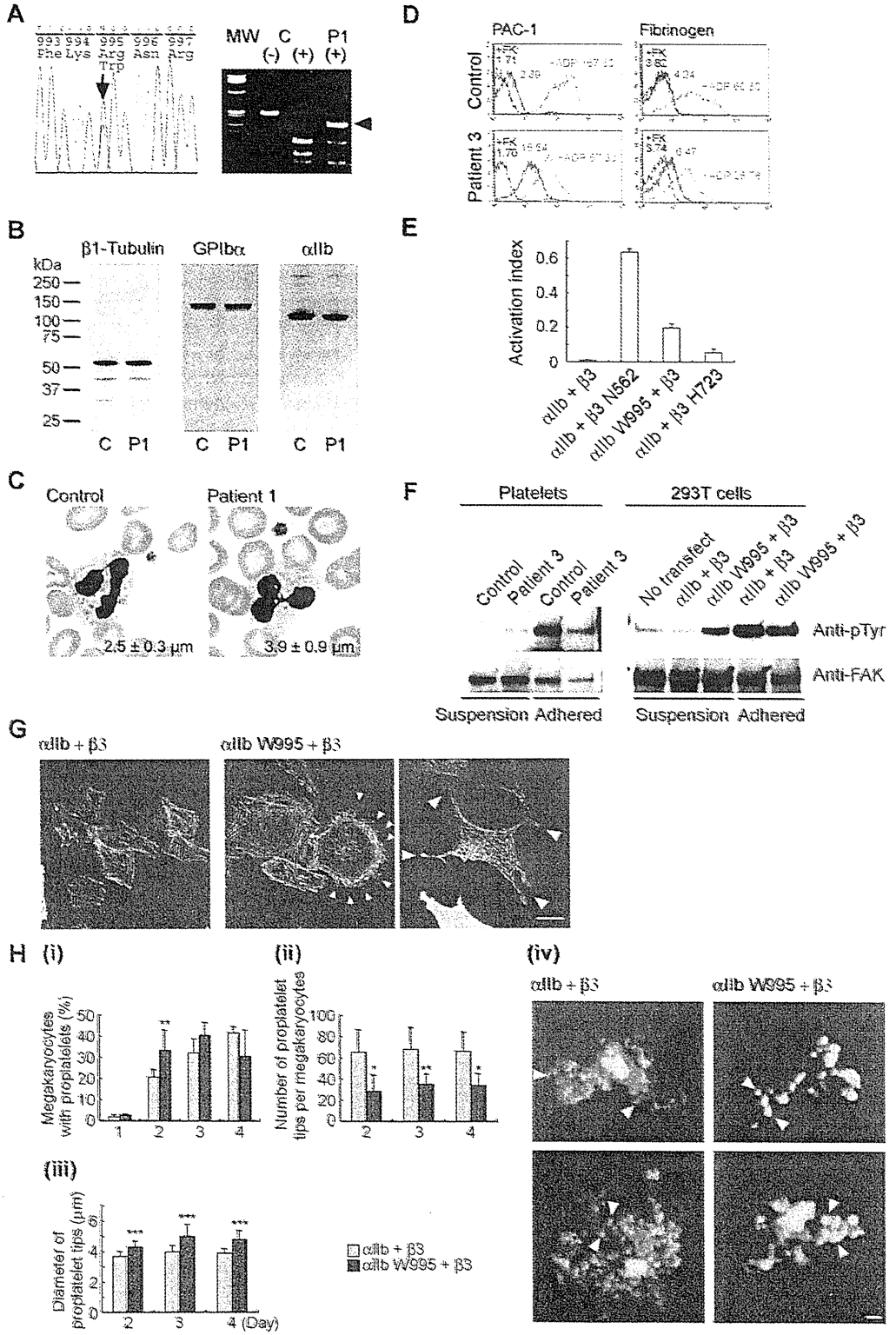

Figure 1. Platelet morphology and biochemical, genetic, and functional analyses of *ITGA2B* R995W mutation. (A: left) DNA sequence analysis of *ITGA2B*. The entire coding regions of the patients' *ITGA2B* were amplified from genomic DNA by the polymerase chain reaction, and amplified DNA fragments were subjected to direct cycle sequence analysis. A C to T transition at nucleotide 3077, changing Arg995 to Trp (R995W), was detected. Nucleotide numbering for *ITGA2B* cDNA is according to Poncz et al.[18] The arrow shows the position of the substitution. (Right) Allele-specific restriction analysis. DNA fragments amplified using primers 2Bg305/303 (supplemental Table 1) were digested with BspACI (SibEnzyme), electrophoresed on 2% agarose gels, and stained with ethidium bromide. The 3077C > T substitution abolishes a recognition site for BspACI, generating a new 231-bp band (arrowhead). The mutation was not found in 108 healthy controls or in the SNP database (www.ncbi.nlm.nih.gov/SNP). MW indicates HaeIII digest of ΦX 174 DNA; C, control; and P1, patient 1. (B) Immunoblot analysis of platelets. Triton X-100-soluble platelet lysates were separated by sodium dodecyl sulfate-polyacrylamide gel electrophoresis on 4% to 12% gradient acrylamide slab gels (Invitrogen) and electroblotted onto polyvinylidine difluoride membranes. The blots were incubated with anti-β1 tubulin antibody NB2301,[19] anti-GPIbα antibody PL524 (Takara), and anti-αIIb antibody SZ22 (Beckman-Coulter) and reacted with horseradish peroxidase-conjugated secondary antibody. The bound antibodies were visualized using an enhanced chemiluminescent substrate. C indicates control; and P1, patient 1.

Transfected cells were subjected to flow cytometry, FAK phosphorylation, and spreading assay.[13,14]

ITGA2B and *ITGB3* cDNAs were inserted upstream of internal ribosome entry site (IRES)-enhanced green fluorescent protein (EGFP) and IRES-Kusabira-Orange in the retroviral vector pGCDNsamIRES/EGFP and pGCDNsamIRES/huKO, respectively.[15,16] Each plasmid was transfected into 293gp packaging cells with a vesicular stomatitis virus G expression plasmid. Supernatants were used for the transduction of 293gpg producer cells harboring a tetracycline-inducible vesicular stomatitis virus G expression cassette,[17] and virus-bearing supernatant was harvested under tetracycline-deficient conditions.

Mouse fetal liver cells were harvested from embryonic day 13.5 embryos and cultured in Dulbecco modified Eagle medium supplemented with 10% fetal calf serum and 50 ng/mL human thrombopoietin. The next day, cells were infected with retroviruses expressing *ITGA2B* and *ITGB3* on recombinant human fibronectin fragment CH-296 (RetroNectin, Takara)-coated plates. After transduction, proplatelet formation was monitored for the next 4 days on EGFP and Kusabira-Orange double-positive megakaryocytes in suspension by inverted fluorescence microscopy. The Experimental Animal Committee of Nagoya Medical Center approved the animal studies.

Results and discussion

We searched for *ITGA2B* and *ITGB3* mutations in 27 patients with macrothrombocytopenia and identified a novel, conserved heterozygous *ITGA2B* R995W mutation in one patient (patient 1; Figure 1A). The decreased surface expression of platelet αIIbβ3 prompted us to prospectively screen its expression by flow cytometry. We detected decreased αIIbβ3 expression level (50%-70% of control) in 3 of 55 consecutive patients with macrothrombocytopenia of unknown etiology (patients 2-4 in Table 1). Immunoblotting showed a normal electrophoretic mobility of αIIb, but the total expression level relative to β1-tubulin was decreased to 0.7 (Figure 1B; Table 1). Sequence analysis identified the same heterozygous *ITGA2B* R995W mutation. In total, we identified 11 patients in 4 unrelated Japanese families. In each family, the disease-associated *ITGA2B* haplotype was unique, indicating independent occurrence (supplemental Table 2). Patients had larger platelets, approximately 30% increase of control, and moderate thrombocytopenia (Figure 1C; Table 1). These results indicate that macrothrombocytopenia shows a dominant inheritance.

Bleeding tendency was absent or mild (eg, patient 1 had undergone total colectomy without platelet transfusion). Platelet aggregation induced by adenosine diphosphate and collagen was reduced, although the bleeding time was within the normal limit (Table 1). Platelet spreading on immobilized fibrinogen was partially impaired: the number of fully spread platelets was decreased (supplemental Figure 1). These findings indicate that patients are asymptomatic or exhibit a marginal bleeding tendency and that the clinical and laboratory phenotype is distinct from Glanzmann thrombasthenia.

There was spontaneous PAC-1 binding to resting patients' platelets as well as to αIIb-W995/β3-transfected 293T cells. Although fibrinogen did not bind to platelets in whole blood, increased fibrinogen binding to the washed platelets was observed (Figure 1D; supplemental Figure 2). The activation state, quantified as an activation index in 293T cells, was higher for αIIb-W995 than for β3-H723 but was weaker than that for a strong activating mutant, β3-N562[13](Figure 1E). CD62p expression was absent on the resting platelets (supplemental Figure 2). Spontaneously phosphorylated FAK, a downstream effector of integrin signaling, was not evident in resting platelets in suspension, probably because of low expression level of abnormal αIIbβ3 receptor. However, FAK phosphorylation occurred in αIIb-W995/β3-transfected 293T cells in suspension, indicating constitutively activated αIIbβ3 (Figure 1F). These results indicate that R995W mutation changes αIIbβ3 to a constitutively, albeit partially, activated conformation, but does not induce platelet activation.

αIIb-R995 forms a salt bridge with β3-D723 in the membrane-proximal region and maintains the inactive conformation of the αIIbβ3.[20,21] Disruption of the interaction because of partially activated αIIb/β3-H723 or αIIb/β3-A723 mutants but not fully activated mutants, such as αIIb/β3-N562, was reported to cause microtubule-dependent abnormal proplatelet-like cytoplasmic extensions in megakaryocytes and CHO cells.[8,22] We found that

Figure 1. (continued) (C) Platelet morphology. Peripheral blood smears were stained with May-Grünwald-Giemsa for a normal control and patient 1 (original magnification, × 1000). The patient showed giant platelets with morphologically normal leukocytes. The number in each panel shows the mean platelet size (n = 200). Images were obtained using a BX50 microscope with a 100×/1.35 numeric aperture oil objective (Olympus). Images of the slides were acquired using a DP70 digital camera and DP manager software Version 1.2.1.107 (Olympus). (D) Activation state of platelet αIIbβ3. Washed platelets from patient 3 were resuspended in Tyrode buffer (137mM NaCl, 2.7mM KCl, 1.0mM $MgCl_2$, 3.3mM NaH_2PO_4, 3.8mM N-2-hydroxyethylpiperazine-N'-2-ethanesulfonic acid, 0.1% glucose, 0.1% bovine serum albumin, pH 7.4) and incubated with fluorescein isothiocyanate-conjugated PAC-1 or 125 μg/mL fluorescein isothiocyanate-labeled fibrinogen in the presence or absence of 10μM FK633 (αIIbβ3-specific peptidomimetic antagonist: black lines) or 10μM adenosine diphosphate (blue lines), and analyzed by flow cytometry. Numbers indicate the mean fluorescence intensity. Results are representative of 2 independent experiments. (E) Quantitation of the αIIbβ3 activation state. The activation state of αIIbβ3 was quantified as an activation index on transiently transfected 293T cells. The activation index was higher for αIIb-W995 than for β3-H723 but was weaker than for an activating mutant β3-N562. Activation index = (a − b)/(c − b), in which a is the mean fluorescence intensity of PAC-1 binding with buffer, b is the mean fluorescence intensity in the presence of FK633, and c is the mean fluorescence intensity in the presence of PT25–2 (anti-αIIbβ3 antibody, which induces the active conformation of αIIbβ3). Data are mean plus or minus SE (n = 3). (F) FAK phosphorylation. Washed platelets from patient 3 (left) or transiently transfected 293T cells (right) were incubated in suspension or seeded onto 100-μg/mL fibrinogen-coated plastic dishes for 1 hour. Cells were washed with phosphate-buffered saline and lysed with 1% Triton X-100 and 1mM sodium vanadate. FAK was immunoprecipitated from the lysates with anti-FAK antibody FAK(C903; Santa Cruz Biotechnology) and protein G-Sepharose, and phosphotyrosine was detected with the antiphosphotyrosine antibody 4G10 (Millipore). Note that 300-μg and 150-μg lysates from suspension and adhered platelets, respectively, and 200-μg lysates from suspension and adhered transfected 293T cells were used for immunoprecipitation analysis. To monitor the loading of gel lanes, the membrane was stripped and reprobed with the anti-FAK antibody FAK(A17; Santa Cruz Biotechnology). Results are representative of 2 and 3 independent experiments for platelets and transfected cells, respectively. (G) Abnormal cytoplasmic protrusions in αIIb-W995/β3-transfected CHO cells. Stably transfected CHO cells were seeded onto 100 μg/mL fibrinogen-coated glass coverslips and incubated for 2 hours at 37°C. Cells were fixed with 3.7% formaldehyde and permeabilized with 0.2% Triton X-100. Coverslips were then stained with anti-CD41a antibody HIP8 (BD Biosciences) followed by Alexa-488-labeled goat antimouse IgG (Invitrogen) and tetramethylrhodamine isothiocyanate-phalloidin (Sigma-Aldrich). Images were obtained using a confocal microscope with a Plan-Apochromat 63×/1.4 oil DIC objective lens LSM5Pascal (Carl Zeiss). Arrowheads indicate membrane ruffling (middle panel) and abnormal cytoplasmic protrusions with the bulbous tips (right panel) in αIIb-W995/β3-transfected CHO cells. Representative images from 3 independent experiments are shown. (H) Abnormal proplatelet formation in αIIb-W995/β3-transfected megakaryocytes. Mouse fetal liver-derived megakaryocytes infected with EGFP-αIIb and Kusabira-Orange-β3 retrovirus were examined in suspension cultures under an IX71 fluorescence microscope with an LCPlanFl 40×/0.60 objective lens (Olympus). (i) The percentage of megakaryocytes extending proplatelets was evaluated manually under a fluorescence microscope 1 to 4 days after infection. For each specimen, at least 100 megakaryocytes were evaluated. The number of proplatelet tips per megakaryocyte (ii) and the size of the proplatelet tips (iii) were measured on acquired images by the ImageScope software Version 10.2.2 (Aperio Technologies). At least 10 megakaryocytes were analyzed for each sample. An unpaired, 2-tailed *t* test was used to analyze data. A value of *P* less than .05 was considered statistically significant. Data are mean plus or minus SD. $^*P < .05$. $^{**}P < .01$. $^{***}P < .0001$. (iv) Representative megakaryocytes from 3 independent experiments are shown. Note that the number of proplatelet tips/bulbous structures (arrowheads) is decreased and the size of the tips increased in αIIb-W995/β3-transfected megakaryocytes than in wild-type αIIb/β3-transfected megakaryocytes. Scale bar represents 10 μm.

Table 1. Platelet characteristics of patients with the *ITGA2B* R995W mutation

Patient	Sex	Age, y	*ITGA2B* mutation	Platelet count, × 10^9/L*	Platelet size, μm†	Surface expression relative to control platelets, %‡					αIIb/β1 tubulin ratio to controls§	Duke bleeding time, minutes‖	Platelet aggregation¶			Bleeding tendency	Initial diagnosis
						αIIb	β3	αIIbβ3	GPIbα	GPIX			ADP, %	Collagen (2.0 μg/mL), %	Ristocetin (1.3 mg/mL), %		
Family 1																	
Patient 1	Male	55	R995W	65	3.9 ± 0.9	53.8	67.0	—	143.1	143.8	0.82	4.5	11 (3μM)	28	77	–	Unknown thrombocytopenia
Family 2																	
Father	Male	46	R995W	79	3.3 ± 0.9	51.3	51.4	56.5	106.7	109.8	—	—	—	—	—	–	—
Patient 2	Male	4	R995W	82	3.6 ± 1.0	54.0	58.6	61.8	138.3	134.7	0.75	5	—	—	—	Epistaxis	Congenital thrombocytopenia
Sister	Female	9	R995W	85	3.4 ± 1.0	55.6	60.6	68.4	120.0	133.1	0.71	3.5	—	—	—	–	—
Family 3																	
Mother	Female	56	R995W	80	2.8 ± 0.8	58.4	63.4	65.8	116.5	—	0.73	—				–	—
Patient 3	Female	27	R995W	74	3.5 ± 1.0	64.4	69.7	63.8	124.8	—	—	—	43 (10μM)	44	72	–	cITP
Sister	Female	24	R995W	100	3.6 ± 1.0	59.3	70.2	70.8	110.9	—	0.63	—	—	—	—	–	—
Family 4																	
Maternal grandfather	Male	58	R995W	66	3.4 ± 0.9	—	—	—	—	—	0.63	—	20 (3μM)	9	—	Hemorrhage in exodontia	—
Mother	Female	30	R995W	66	2.8 ± 0.8	56.3	62.5	57.5	127.2	112.1	0.63	2.5	—	—		Purpura, hemorrhage in exodontia	cITP
Patient 4	Female	4M	R995W	82	3.2 ± 1.0	63.3	62.9	62.3	147.7	140.5	0.63	—	23 (3μM)	11	—	–	NAITP
Brother	Male	5	R995W	122	3.1 ± 0.8	—	—	—	—	—	—	—	—	—	—	–	—
Mean + SD				81.9 + 16.8#	3.3 + 0.3#	57.4 + 4.4**	62.9 + 5.8**	63.3 + 5.0**	126.1 + 14.3**	129.0 + 14.5**	0.7 + 0.07#						

— indicates not applicable; ADP, adenosine diphosphate; cITP, chronic immune thrombocytopenia; and NAITP, neonatal alloimmune thrombocytopenic purpura.

*Controls, 273.5 ± 60.4 (× 10^9/L) (n = 1014).

†Determined by microscopic observation of 200 platelets on a stained peripheral blood smear. Controls, 2.5 ± 0.3 μm (n = 31).

‡Platelets were reacted with fluorescein isothiocyanate-labeled monoclonal antibodies against αIIb (5B12; Dako Denmark), β3 (SZ21), αIIbβ3 (P2), GPIbα (SZ2; Beckman-Coulter), or GPIX (ALMA16; BD Biosciences) and analyzed in an Epics XL flow cytometer (Beckman-Coulter). Values are expressed as percentage of mean fluorescence intensities of control platelets.

§Platelet αIIb/β1-tubulin ratio was determined by densitometric analysis of immunoblots using ImageQuant software Version 5.0 (Molecular Dynamics).

‖Normal range, 2 to 5 minutes.

¶Platelet aggregation was performed in platelet-rich plasma. Results are given as percentage maximum aggregation.

#$P < .001$, **$P < .0001$ vs controls (2-tailed t test).

αIIb-W995/β3-transfected CHO cells exhibited membrane ruffling and abnormal cytoplasmic protrusions with the bulbous tips on fibrinogen-coated surfaces (Figure 1G), indicating that the salt bridge-disrupting mutations exert the same influence on the integrin activation and cytoskeletal events. Abnormal clustering of αIIbβ3, which was reported in *ITGB3* L718P mutation,[10] was not observed in these cells or in platelets spread on immobilized fibrinogen (supplemental Figure 1). It is worth noting that macrothrombocytopenia-associated *ITGB3* mutations in the ectodomain and the cytoplasmic membrane-proximal region have different properties in terms of outside-in signaling and bleeding tendency.[9,10]

Finally, to determine the functional consequences of R995W mutation on platelet production, we coexpressed αIIb and β3 in mouse fetal liver cells by retroviral transfer and differentiated them into megakaryocytes (Figure 1H). There was an early increase and decrease in the percentage of proplatelet formation-positive megakaryocytes in αIIb-W995/β3-transfected megakaryocytes. The number of proplatelet tips was decreased, and the size of the tips increased. These results are consistent with thrombocytopenia and the increased platelet size in patients, indicating that the stimulation of mutant αIIbβ3 leads to abnormal proplatelet formation. However, not all *ITGA2B*- and *ITGB3*-activating mutations are associated with macrothrombocytopenia. Patients with homozygous *ITGB3* C549R or C560R mutation inducing constitutively active αIIbβ3 have a normal platelet count and size,[23,24] suggesting different molecular mechanisms for the induction of abnormal proplatelet formation.

αIIbβ3 has not been implicated in an abnormal platelet count or morphology.[5] Our data support and extend the recent reports that heterozygous, activating mutations in *ITGA2B* and *ITGB3*, in the juxtamembrane region, cause macrothrombocytopenia.[6-10] We thus propose that such mutations represent the etiology of a subset of congenital macrothrombocytopenias. It is also probable that homozygosity causes Glanzmann thrombasthenia, as demonstrated in the original report of macrothrombocytopenia-associated *ITGA2B* R995Q mutation.[6,7] The creation of a knock-in mouse model and/or use of an in vivo megakaryocyte infusion model[25] should clarify the mechanism underlying the production and processing of giant platelets.

Acknowledgments

The authors thank Dr R. C. Mulligan (Children's Hospital Boston, Harvard Medical School, Boston, MA) for 293gp and 293gpg cells, Dr M. Handa (Department of Transfusion Medicine & Cell Therapy, Keio University School of Medicine, Tokyo, Japan) for PT25-2 antibodies, Dr A. Saito (Department of Clinical Research Promotion, Clinical Research Center, National Hospital Organization Nagoya Medical Center) for statistical analysis, and Yoshimi Ito-Yamamura for her skillful technical assistance.

This work was supported by the Japan Society for the Promotion of Science (Grant-in-Aid for Scientific Research), the Ministry of Health, Labor and Welfare, Academic Frontier Project in Japan, Mitsubishi Pharma Research Foundation, the 24th General Assembly of the Japanese Association of Medical Sciences Promotion Fund, the Mother and Child Health Foundation, and the National Hospital Organization Research Fund.

Authorship

Contribution: S.K. designed and performed research, analyzed data, and wrote the paper; H.K. and Y. Tomiyama performed platelet experiments and interpreted the results; M. Onodera constructed retrovirus vectors; M. Otsu, N.T., K.E., and M. Onodera designed the retroviral transfection experiments; Y.M., Y. Takamatsu, J.S., and K.M. contributed patient samples; and H.S. supervised the research.

Conflict-of-interest disclosure: The authors declare no competing financial interests.

Correspondence: Shinji Kunishima, Department of Advanced Diagnosis, Clinical Research Center, National Hospital Organization Nagoya Medical Center, 4-1-1 Sannomaru, Naka-ku, Nagoya 4600001, Japan; e-mail: kunishis@nnh.hosp.go.jp.

References

1. Balduini CL, Cattaneo M, Fabris F, et al. Inherited thrombocytopenias: a proposed diagnostic algorithm from the Italian Gruppo di Studio delle Piastrine. *Haematologica.* 2003;88(5):582-592.
2. Balduini CL, Savoia A. Inherited thrombocytopenias: molecular mechanisms. *Semin Thromb Hemost.* 2004;30(5):513-523.
3. Kunishima S, Saito H. Congenital macrothrombocytopenias. *Blood Rev.* 2006;20(2):111-121.
4. Nurden P, Nurden AT. Congenital disorders associated with platelet dysfunctions. *Thromb Haemost.* 2008;99(2):253-263.
5. Nurden AT. Glanzmann thrombasthenia. *Orphanet J Rare Dis.* 2006;1:10.
6. Hardisty R, Pidard D, Cox A, et al. A defect of platelet aggregation associated with an abnormal distribution of glycoprotein IIb-IIIa complexes within the platelet: the cause of a lifelong bleeding disorder. *Blood.* 1992;80(3):696-708.
7. Peyruchaud O, Nurden AT, Milet S, et al. R to Q amino acid substitution in the GFFKR sequence of the cytoplasmic domain of the integrin IIb subunit in a patient with a Glanzmann's thrombasthenia-like syndrome. *Blood.* 1998;92(11):4178-4187.
8. Ghevaert C, Salsmann A, Watkins NA, et al. A nonsynonymous SNP in the ITGB3 gene disrupts the conserved membrane-proximal cytoplasmic salt bridge in the alphaIIbbeta3 integrin and co-segregates dominantly with abnormal proplatelet formation and macrothrombocytopenia. *Blood.* 2008;111(7):3407-3414.
9. Gresele P, Falcinelli E, Giannini S, et al. Dominant inheritance of a novel integrin beta3 mutation associated with a hereditary macrothrombocytopenia and platelet dysfunction in two Italian families. *Haematologica.* 2009;94(5):663-669.
10. Jayo A, Conde I, Lastres P, et al. L718P mutation in the membrane-proximal cytoplasmic tail of beta3 promotes abnormal alphaIIbbeta3 clustering and lipid microdomain coalescence, and associates with a thrombasthenia-like phenotype. *Haematologica.* 2010;95(7):1158-1166.
11. Kunishima S, Hamaguchi M, Saito H. Differential expression of wild-type and mutant NMMHC-IIA polypeptides in blood cells suggests cell-specific regulation mechanisms in MYH9 disorders. *Blood.* 2008;111(6):3015-3023.
12. Kunishima S, Lopez JA, Kobayashi S, et al. Missense mutations of the glycoprotein (GP) Ibbeta gene impairing the GPIb alpha/beta disulfide linkage in a family with giant platelet disorder. *Blood.* 1997;89(7):2404-2412.
13. Kashiwagi H, Tomiyama Y, Tadokoro S, et al. A mutation in the extracellular cysteine-rich repeat region of the beta3 subunit activates integrins alphaIIbbeta3 and alphaVbeta3. *Blood.* 1999;93(8):2559-2568.
14. Kashiwagi H, Shiraga M, Kato H, et al. Expression and subcellular localization of WAVE isoforms in the megakaryocyte/platelet lineage. *J Thromb Haemost.* 2005;3(2):361-368.
15. Sanuki S, Hamanaka S, Kaneko S, et al. A new red fluorescent protein that allows efficient marking of murine hematopoietic stem cells. *J Gene Med.* 2008;10(9):965-971.
16. Suzuki A, Obi K, Urabe T, et al. Feasibility of ex vivo gene therapy for neurological disorders using the new retroviral vector GCDNsap packaged in the vesicular stomatitis virus G protein. *J Neurochem.* 2002;82(4):953-960.
17. Ory DS, Neugeboren BA, Mulligan RC. A stable human-derived packaging cell line for production of high titer retrovirus/vesicular stomatitis virus G pseudotypes. *Proc Natl Acad Sci U S A.* 1996;93(21):11400-11406.
18. Poncz M, Eisman R, Heidenreich R, et al. Structure of the platelet membrane glycoprotein IIb: homology to the alpha subunits of the vitronectin and fibronectin membrane receptors. *J Biol Chem.* 1987;262(18):8476-8482.

19. Kunishima S, Kobayashi R, Itoh TJ, Hamaguchi M, Saito H. Mutation of the beta1-tubulin gene associated with congenital macrothrombocytopenia affecting microtubule assembly. *Blood.* 2009;113(2):458-461.

20. Hughes PE, Diaz-Gonzalez F, Leong L, et al. Breaking the integrin hinge: a defined structural constraint regulates integrin signaling. *J Biol Chem.* 1996;271(12):6571-6574.

21. Lau TL, Kim C, Ginsberg MH, Ulmer TS. The structure of the integrin alphaIIbbeta3 transmembrane complex explains integrin transmembrane signalling. *EMBO J.* 2009;28(9):1351-1361.

22. Schaffner-Reckinger E, Salsmann A, Debili N, et al. Overexpression of the partially activated alphaIIbbeta3D723H integrin salt bridge mutant downregulates RhoA activity and induces microtubule-dependent proplatelet-like extensions in Chinese hamster ovary cells. *J Thromb Haemost.* 2009;7(7):1207-1217.

23. Mor-Cohen R, Rosenberg N, Peretz H, et al. Disulfide bond disruption by a beta3-Cys549Arg mutation in six Jordanian families with Glanzmann thrombasthenia causes diminished production of constitutively active alphaIIbbeta3. *Thromb Haemost.* 2007;98(6):1257-1265.

24. Ruiz C, Liu CY, Sun QH, et al. A point mutation in the cysteine-rich domain of glycoprotein (GP) IIIa results in the expression of a GPIIb-IIIa (alphaIIbbeta3) integrin receptor locked in a high-affinity state and a Glanzmann thrombasthenia-like phenotype. *Blood.* 2001;98(8):2432-2441.

25. Fuentes R, Wang Y, Hirsch J, et al. Infusion of mature megakaryocytes into mice yields functional platelets. *J Clin Invest.* 2010;120(11):3917-3922.

Anti-Melanoma Differentiation-Associated Gene 5 Antibody is a Diagnostic and Predictive Marker for Interstitial Lung Diseases Associated with Juvenile Dermatomyositis

Ichiro Kobayashi, MD, PhD, Yuka Okura, MD, Masafumi Yamada, MD, PhD, Nobuaki Kawamura, MD, PhD, Masataka Kuwana, MD, PhD, and Tadashi Ariga, MD, PhD

The presence of the anti-melanoma differentiation-associated gene 5 antibody was evaluated in 13 patients with juvenile dermatomyositis (JDM). The antibody was positive in 5 of the 6 patients with JDM-associated interstitial lung disease (ILD), but not in the 7 patients without ILD. This antibody is a useful marker for early diagnosis of JDM-associated ILD. *(J Pediatr 2011;158:675-7)*

Juvenile dermatomyositis (JDM) is a rare disease characterized by skin erythema and muscle involvement associated with vasculopathy.[1] Interstitial lung disease (ILD) is a common complication of adult dermatomyositis (DM) and is often rapidly progressive when complicating clinically amyopathic DM (CADM).[2] Although pulmonary function is impaired in most of cases of JDM, confirmation of ILD by imaging is rare.[1,3,4] Once ILD develops, however, it progresses rapidly at an early stage or during relapse of JDM and necessitates early intensive immunosuppressive therapy with cyclosporine A (CSA).[4] Recently, anti-melanoma differentiation-associated gene 5 (MDA5) antibody was identified as a disease marker for adult CADM-associated rapidly progressive ILD (RP-ILD).[5] In the present study, we examined this autoantibody in children with JDM-associated ILD.

Methods

Thirteen patients with JDM followed up at Hokkaido University Hospital and Kitami Red Cross Hospital between April 1990 and March 2010 were retrospectively reviewed and enrolled in this study. The diagnosis of JDM was made according to the diagnostic criteria of Bohan and Peter.[6] Amyopathic JDM was diagnosed according to the diagnostic criteria of Gerami et al.[7] Serum KL-6 levels were routinely monitored at least once a month since 2000 or tested for stored sera from patients before 1999.[3] Chest x-ray and computed tomography (CT) scan and pulmonary function tests were performed at the time of diagnosis of JDM, onset of respiratory symptoms, relapse of JDM, and detection of an elevated serum KL-6 level.

All serum samples were obtained at the time of diagnosis of JDM and stored at -20°C until analysis. Anti-MDA5 antibody was measured by enzyme-linked immunosorbent assay as described previously.[5] The number of antibody units was calculated from the optical density at 450 nm results (normal range, <8 U).[5]

Results

Clinical and laboratory features of the patients with JDM-associated ILD are presented in the **Table**. Patients 1-5 have been reported previously.[3,4] ILD progressed rapidly despite treatment with methylprednisolone pulse therapy (mPSL) in 3 patients. In patients 3 and 6, abnormal CT findings were not observed at the time of diagnosis of JDM but developed later in association with elevated serum KL-6 level. Patient 1 died of respiratory failure, but the other 5 patients recovered after the commencement of CSA therapy (3-5 mg/kg/day) in combination with repeated mPSL pulse therapy (15-30 mg/kg/day for 3 consecutive days) and oral high-dose prednisolone (1-2 mg/kg/day, maximum dose of 60 mg/day). After complete resolution of abnormal chest CT scan findings and serum muscle-derived enzyme levels, the prednisolone and CSA doses were gradually decreased. Four patients have been drug-free for at least 4 years without relapse of either JDM or ILD. All of the patients with ILD exhibited clinical myositis associated with elevated levels of serum muscle-derived enzymes early in the disease. Of the 7 patients without ILD (5 males and 2 females, aged 2-12 years), 2 females were diagnosed with amyopathic JDM.

CADM	Clinically amyopathic dermatomyositis
CSA	Cyclosporine A
CT	Computed tomography
DM	Dermatomyositis
ILD	Interstitial lung disease
JDM	Juvenile dermatomyositis
MDA5	Anti-melanoma differentiation-associated gene 5
mPSL	Methylprednisolone pulse therapy
RP-ILD	Rapidly progressive interstitial lung disease

From the Department of Pediatrics, Hokkaido University Graduate School of Medicine, Sapporo, Japan (I.K., Y.O., M.Y., T.A.); Department of Pediatrics, Sapporo City General Hospital, Sapporo, Japan (N.K.); and Department of Rheumatology, Keio University School of Medicine, Tokyo, Japan (M.K.)

Supported in part by the Ministry of Health, Labor, and Welfare of Japan. The authors declare no conflicts of interest.

 10.1016/j.jpeds.2010.11.033

Table. Profiles of the patients with JDM-associated ILD

	Patient					
	1	2	3	4	5	6
Age of onset, years	8	14	4	10	14	7
Sex	M	M	F	F	F	M
Complication	RP-ILD, pneumothorax	ILD, HPS, skin ulcer	ILD	ILD, thrombocytopenia	RP-ILD, thrombocytopenia	RP-ILD, skin ulcer
Onset of ILD, months*	2	1	7†	1	1	1
% vital capacity‡	22.3%	66.6%	ND	56.0%	56.9%	61.8%
CSA therapy, months§	1	3	1	3	0	0
CK (IU/L)¶	1250	249	69	2112	1435	348
AST (IU/L)¶	443	559	112	1363	244	228
Aldolase (IU/L)¶	9.6	24.7	15.5	16.5	20.5	20.0
KL-6 (U/mL)¶	2460	2096	1091	1430	1695	2376
Treatment	mPSL, PSL, AZA, CSA	mPSL, PSL, IVIG, CSA	mPSL, PSL, CSA	mPSL, PSL, CSA	mPSL, PSL, IVIG, CSA	mPSL, PSL, CSA
Response of ILD to mPSL	Poor	Poor	Partial	Partial	Poor	Poor
Outcome	Died	Remission	Remission	Remission	Remission	Under treatment

Normal reference values: CK, 30-165 IU/L; AST, 5-40 IU/L; aldolase, 2.0-4.8 IU/L; KL-6, <500 U/mL.
AST, aspartate aminotransferase; *AZA*, azathiopurine; *CK*, creatine phosphokinase; *HPS*, hemophagocytic syndrome; *IVIG*, intravenous immunoglobulin; *PSL*, prednisolone.
*Onset of ILD after the diagnosis of JDM.
†ILD developed on relapse of JDM.
‡Lowest values in the course.
§Commencement of CSA after the onset of ILD.
¶Maximum values in the course.

Five of the 6 patients with ILD were positive for the anti-MDA5 antibody (9.5-902.3 U) (**Figure**). Three patients with RP-ILD (patients 1, 5, and 6) had extremely high levels of the antibody (357.6-902.3 U). Two patients with delayed development of ILD were positive for the antibody at the time of diagnosis of JDM. All of the 7 patients without ILD were negative for the antibody (1.3-3.5 U).

Discussion

This retrospective study involved only a small number of cases, given the rarity of ILD in JDM. Nevertheless, anti-MDA5 antibody was both sensitive and specific for JDM-associated ILD, as has been reported in adult cases.[5] Because serum levels of KL-6, a marker for ILD,[3] are increased in other life-threatening diseases, such as *Pneumocystis* infection, patients with an elevated KL-6 level require further evaluation by CT scan. The anti-MDA5 antibody could be useful for the differential diagnosis in such cases. Three patients with RP-ILD had particularly high titers of the antibody. In contrast to adult cases, all of the antibody-positive cases exhibited muscle weakness and elevated levels of muscle-derived enzymes during the course of the disease. Of note, anti-MDA5 antibody was positive before the onset of ILD in 2 cases, suggesting that the presence of the antibody predicts the development of RP-ILD.

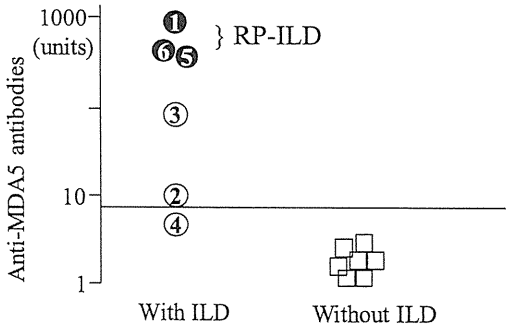

Figure. Enzyme-linked immunosorbent assay of serum anti-MDA5 antibody in JDM. The antibody units of the sera from 13 patients with JDM with and without interstitial lung disease are displayed. Numbers in the circles represent the patients. The horizontal line represents the cutoff value (8.0 units).

MDA5 acts as a sensor for double-strand RNAs of viruses such as coxsackievirus, which have been implicated in the development of JDM, and induces type I interferon, a potent stimulator of B, T, and natural killer cells.[1,8] Indeed, type I interferon produced by plasmacytoid dendritic cells as well as by B and $CD4^+$ T cells plays a critical role in the pathogenesis of myositis in JDM.[1] On the other hand, analyses of bronchoalveolar lavage fluid have found an elevated ratio of $CD4^+/CD8^+$ T cells and increased numbers of activated $CD8^+$ $HLA\text{-}DR^+$ cells, suggesting pathological roles of T cells in adult CADM-associated RP-ILD.[2,9] In addition, antigen-specific proliferation of T cells is suggested by restricted usage of T cell receptor $V\beta$ genes in both muscular and pulmonary lesions of DM.[10] Given that the autoantigens identified by the reactivity with autoantibodies also stimulate self-reactive T cells, MDA5 could be a target of T cells and involved in the development of ILD. The antibody assay was negative in 2 patients with acute lupus pneumonitis or systemic sclerosis associated with pulmonary fibrosis (data not shown), suggesting different mechanisms of ILD in JDM and other collagen vascular diseases.

Two survivors with RP-ILD in our series received CSA in combination with mPSL pulse therapy within 3 weeks after the diagnosis of ILD, whereas the commencement of CSA therapy was delayed in another patient with RP-ILD, who

died of respiratory failure. Early intervention with the combination of a corticosteroid and CSA has been associated with improved outcome in adult CADM-associated RP-ILD.[11] JDM-associated ILD is similar to adult CADM-associated RP-ILD in both pathogenesis and response to treatment, as well as in the presence of the anti-MDA5 antibody.

In conclusion, our findings suggest that anti-MDA5 autoantibody could serve not only as a disease marker of ILD associated with JDM, but also as a predictive marker for the complication of ILD. Cases of JDM with a high titer of the antibody are associated with RP-ILD in particular and necessitate early intensive therapy. ■

Submitted for publication Sep 4, 2010; last revision received Oct 22, 2010; accepted Nov 15, 2010.

Reprint requests: Ichiro Kobayashi, MD, PhD, Department of Pediatrics, Hokkaido University Graduate School of Medicine, North-15 West-7, Sapporo, 060-8638 Japan. E-mail: ichikobaya@med.hokudai.ac.jp

References

1. Feldman BM, Rider LG, Reed AM, Pachman LM. Juvenile dermatomyositis and other idiopathic inflammatory myopathies of childhood. Lancet 2008;371:2201-12.
2. Mukae H, Ishimoto H, Sakamoto N, Hara S, Kakugawa T, Nakayama S, et al. Clinical differences between interstitial lung disease associated with clinically amyopathic dermatomyositis and classical dermatomyositis. Chest 2009;136:1341-7.
3. Kobayashi I, Ono S, Kawamura N, Okano M, Miyazawa K, Shibuya H, et al. A serum level of KL-6 is a marker for interstitial lung disease associated with juvenile dermatomyositis. J Pediatr 2001;138:274-6.
4. Kobayashi I, Yamada M, Takahashi Y, Kawamura N, Okano M, Sakiyama Y, et al. Interstitial lung disease associated with juvenile dermatomyositis; clinical features and efficacy of cyclosporine A. Rheumatology 2003;43:371-4.
5. Sato S, Hoshino K, Satoh T, Fujita T, Kawakami Y, Fujita T, et al. RNA helicase encoded by melanoma differentiation-associated gene 5 is a major autoantigen in patients with clinically amyopathic dermatomyositis: association with rapidly progressive interstitial lung disease. Arthritis Rheum 2009;60:2193-200.
6. Bohan A, Peter JB. Polymyositis and dermatomyositis. N Engl J Med 1975;292:344-7.
7. Gerami P, Walling HW, Lewis J, Doughty L, Sontheimer RD. A systematic review of juvenile-onset clinically amyopathic dermatomyositis. Br J Dermatol 2007;157:637-44.
8. Kato H, Takeuchi O, Sato S, Yoneyama M, Yamamoto M, Matsui K, et al. Differential roles of MDA5 and RIG-I helicases in the recognition of RNA viruses. Nature 2006;441:101-5.
9. Kourakata H, Takada T, Suzuki E, Enomoto K, Saito I, Taguchi Y, et al. Flowcytometric analysis of bronchoalveolar lavage fluid cells in polymyositis/dermatomyositis with interstitial pneumonia. Respirology 1999;4:223-8.
10. Englund P, Wahlström J, Fathi M, Rasmussen E, Grunewald J, Tornling G, et al. Restricted T cell receptor BV gene usage in the lungs and muscles of patients with idiopathic inflammatory myopathies. Arthritis Rheum 2007;56:372-83.
11. Kotani T, Makino S, Takeuchi T, Kagitani M, Shoda T, Hata A, et al. Early intervention with corticosteroids and cyclosporin A and 2-hour postdose blood concentration monitoring improves the prognosis of acute/subacute interstitial pneumonia in dermatomyositis. J Rheumatol 2008;35:254-9.

ARTHRITIS & RHEUMATISM
Vol. 63, No. 8, August 2011, pp 2465–2472
DOI 10.1002/art.30415

Association of Hepatocyte Growth Factor Promoter Polymorphism With Severity of Interstitial Lung Disease in Japanese Patients With Systemic Sclerosis

Kana Hoshino,[1] Takashi Satoh,[1] Yasushi Kawaguchi,[2] and Masataka Kuwana[1]

Objective. To examine associations of single-nucleotide polymorphisms (SNPs) within genes for hepatocyte growth factor (HGF) and its receptor c-*met* with disease susceptibility and organ involvement in Japanese patients with systemic sclerosis (SSc).

Methods. Four SNPs (*HGF* −1652 C/T, +44222 C/T, and +63555 G/T, and c-*met* −980 T/A) were analyzed in 159 SSc patients and 103 healthy control subjects with the use of a polymerase chain reaction–based assay. The influence of the *HGF* −1652 SNP on transcription activity was evaluated with a luciferase reporter assay and an electrophoretic mobility shift assay (EMSA).

Results. There was no difference in the distribution of *HGF*/c-*met* SNPs between SSc patients and controls. *HGF* −1652 TT was found much more frequently in SSc patients with end-stage lung disease (ESLD) than in those without (41% versus 8%; $P = 0.0004$). This association was confirmed by a replication study involving a separate cohort of 155 SSc patients. Kaplan-Meyer analysis revealed that *HGF* −1652 TT carriers had a higher probability of developing ESLD than did CT or CC carriers. The *HGF* promoter carrying the *HGF* −1652 T allele had lower transcription activity than did the promoter carrying the C allele. EMSA showed the presence of a potential negative transcription regulator that binds specifically to the *HGF* promoter carrying a T allele at position −1652. Finally, TT carriers had a relative inability to increase circulating HGF levels even in the presence of advanced interstitial lung disease.

Conclusion. A SNP in the *HGF* promoter region may modulate the severity of interstitial lung disease by controlling the transcriptional efficiency of the *HGF* gene.

Systemic sclerosis (SSc) is a connective tissue disease characterized by fibrosis of the skin and internal organs, microvasculopathy, and the presence of circulating antinuclear antibodies (ANAs). The cause of the disease remains unclear, but both genetic and environmental factors contribute to its development (1). Recent findings indicate that a series of growth factors and cytokines are involved in the pathogenesis of SSc (2). For example, transforming growth factor β (TGFβ) is a profibrotic factor that stimulates fibroblast collagen production and promotes extracellular matrix deposits. Other profibrotic factors include connective tissue growth factor (CTGF) and platelet-derived growth factor.

In contrast, hepatocyte growth factor (HGF), a ligand for the c-*met* receptor tyrosine kinase, is an antifibrotic factor that helps to regenerate damaged tissue by inhibiting fibrosis and promoting angiogenesis (3). A series of studies have shown that HGF suppresses fibrosis by inhibiting collagen production, inducing myofibroblast apoptosis, and degrading the extracellular matrix (4,5). Since HGF counteracts many of the profibrotic actions of TGFβ, it has been proposed that a balance between HGF and TGFβ may play a decisive role in the pathogenesis of fibrosis (6,7). However, patients with SSc have increased circulating levels of HGF as compared to those in healthy controls (8). This level of HGF may not be sufficient to inhibit the ongoing fibrotic process.

Supported by a grant for research on intractable diseases from the Japanese Ministry of Health, Labor, and Welfare and by a grant from the Japanese Ministry of Education, Science, Sports, and Culture.

Kana Hoshino, MSc, Takashi Satoh, PhD, Masataka Kuwana, MD, PhD: Keio University School of Medicine, Tokyo, Japan; Yasushi Kawaguchi, MD, PhD: Tokyo Women's Medical University, Tokyo, Japan.

Address correspondence to Masataka Kuwana, MD, PhD, Division of Rheumatology, Department of Internal Medicine, Keio University School of Medicine, 35 Shinanomachi, Shinjuku-ku, Tokyo 160-8582, Japan. E-mail: kuwanam@z5.keio.jp.

Submitted for publication September 24, 2010; accepted in revised form April 14, 2011.

The prevalence and severity of interstitial lung disease (ILD) in SSc patients varies among ethnic groups. ILD is more common and more progressive in African American than in Caucasian patients (9,10). Even in a relatively homogeneous group of SSc patients with serum anti–topoisomerase I (anti–topo I) antibody, Japanese and African American patients were found to have more-prominent deterioration of lung function and lower survival rates than Caucasian patients (11). Together, these findings suggest that ethnicity influences the onset and progression of SSc-associated ILD, likely through differences in both genetic and environmental backgrounds. A recent study of SSc patients showed that increased HGF levels were observed in bronchoalveolar lavage fluid and plasma samples from Caucasian patients but not African American patients (12), suggesting that ethnic differences in susceptibility to pathologic fibrosis in the lungs may be explained by genetic control of HGF expression.

In this study, we selected single-nucleotide polymorphisms (SNPs) within genes for the *HGF* and c-*met* loci in Japanese patients with SSc and examined their associations with disease susceptibility, organ involvement, and autoantibody profiles. We also examined the underlying mechanism of an association between an *HGF* SNP and ILD outcomes.

PATIENTS AND METHODS

Patients and controls. We studied 159 Japanese SSc patients whose cases were followed between 1988 and 2008 at Keio University Hospital (cohort 1). An additional 155 Japanese patients from Tokyo Women's Medical University Hospital were used as a replication cohort (cohort 2). All patients met the American College of Rheumatology preliminary classification criteria for SSc (13). SSc patients were classified as having diffuse cutaneous SSc (dcSSc) or limited cutaneous SSc (lcSSc) according to the classification described by Medsger (14). Controls included 103 healthy Japanese volunteers residing in the Tokyo metropolitan area.

All samples were obtained after the patients and control subjects had given their written informed consent. The study protocol was approved by the Institutional Review Boards of Keio University and Tokyo Women's Medical University.

Assessment of clinical features. Records of clinical and laboratory findings were kept prospectively for all patients. A complete medical history, physical examination, and laboratory analyses were performed at each patient's first visit, and more-limited evaluations were performed during followup visits (at least once every 3 months). Forced vital capacity (FVC) measured within 3 months before and 3 months after blood collection was used to examine its association with circulating concentrations of HGF. For all patients, any SSc-related major organ involvement was documented, including that of the peripheral vasculature (digital ulcer), esophagus, heart, kidney, lung parenchyma (ILD), and lung vasculature (pulmonary arterial hypertension).

The criteria used to define individual organ involvement have been described elsewhere (15). ILD was defined as the presence of bibasilar reticulation and/or fibrosis on chest radiograph. End-stage lung disease (ESLD) was defined as the presence of at least 1 of the following 3 features: <50% FVC, required oxygen supplementation in the absence of pulmonary arterial hypertension, or death due to ILD-related causes (16).

Identification of SSc-related ANAs. Serum samples from all SSc patients were analyzed for anticentromere, anti–topo I, and anti–U1 small nuclear RNP (anti–U1 snRNP) antibodies, which are major SSc-related ANAs in the Japanese population (15), using indirect immunofluorescence and immunoprecipitation assays (15).

Genotyping of *HGF* and c-*met* SNPs. Based on heterogeneous allelic distribution in the Japanese population (17,18), we selected for analysis 3 SNPs within the *HGF* gene, namely, –1652 (rs3735520) C/T, +44222 (rs2887069) C/T, and +63555 G/T, as well as 1 SNP within the c-*met* gene, –980 (rs38839) T/A. Genomic DNA was isolated from peripheral blood mononuclear cells using a QIAamp DNA Mini kit (Qiagen). Individual SNPs were determined by amplifying genes of interest by polymerase chain reaction (PCR), followed by restriction fragment length polymorphism (RFLP). Table 1

Table 1. RFLP conditions and primers used for analysis of the 4 single-nucleotide polymorphisms within the *HGF* and c-*met* genes*

Gene location	Region	Primer sequence (5′→3′)	Annealing temperature (°C)	Restriction enzyme used for RFLP
HGF –1652 C/T (rs3735520)	Promoter	Sense: CAGACAGAGGCTGACAAATG Antisense: CACTTTCAGGGAAAAACAACCTGC	66.5	*Bsl* I
HGF +44222 C/T (rs2887069)	Intron 9	Sense: GCTGACATTCTGCAGGGTGGGC Antisense: CTCCAGGGGGTCAGATAGCTTAG	68.5	*Alu* I
HGF +63555 G/T	Exon 15	Sense: CCTTCCTGCTTCTCAGCAAGGTCAC Antisense: CGAACTGCCACACAGCTGAAG	66.5	*Ssp* I
c-*met* –980 T/A (rs38839)	Promoter	Sense: CAAGTTGGTATGAGAGCCGGAACG Antisense: GAGGAGTTTAACCCTGAGGAGACT	59.7	*Dra* I

* RFLP = restriction fragment length polymorphism.

shows the primer sequences and annealing temperatures used for PCR, as well as the restriction enzymes used for RFLP. PCR conditions consisted of an initial denaturation at 95°C for 5 minutes, followed by 35 cycles of denaturation at 95°C, annealing at optimal temperature, and extension at 72°C for 30 seconds each cycle, and a final extension step at 72°C for an additional 5 minutes. The PCR products were digested with the corresponding restriction enzymes, separated on a 12% polyacrylamide gel, and stained with ethidium bromide.

Assessment of *HGF* promoter activity. A series of DNA fragments encoding the promoter region of the *HGF* gene were amplified by PCR using genomic DNA samples known to be homozygous for *HGF* −1652 CC or TT as a template. The 5 fragments generated included nucleotides −460 to −1, −831 to −1, −1313 to −1, and −1756 to −1 with a C allele at −1652, and −1756 to −1 with a T allele at −1652. The sense primer sequences were 5′-GGATCCTGGGGACACCAGAC-3′ (−1756 to −1), 5′-ACCAGAGCATCCACCTCTGGG-3′ (−1313 to −1), 5′-GCTGCCTGCTCTGAGCCCAT-3′ (−831 to −1), and 5′-GAATTGGTCCCCTGCCTGTGCCT-3′ (−460 to −1). The amplification antisense primer sequence was 5′-GGTGCTGCTGGACGGGCTGGC-3′. The genotype was verified by sequencing on an ABI Prism 3100 genetic analyzer using a BigDye Terminator Cycle Sequence Ready Reaction kit (both from Applied Biosystems).

HGF promoter activity was measured with a Dual-Luciferase Reporter Assay system (Promega) according to the manufacturer's protocol. Lung squamous cell carcinoma cell line EBC-1 cells were cotransfected with a firefly luciferase plasmid harboring the HGF promoter region and a *Renilla* luciferase reporter plasmid, using Lipofectamine 2000 (Invitrogen). The cells were lysed, and firefly and *Renilla* luciferase activity were each measured with a Micro Lumat Plus LB96V luminometer (Berthold Technologies). The relative *HGF* promoter activity was calculated as the ratio of firefly luciferase activity to *Renilla* luciferase activity as an internal reference. The *HGF* promoter region covering nucleotides −460 to −1 was defined as a basic transcription activation domain (19).

Electrophoretic mobility shift assay (EMSA). The interaction of nuclear factors with the DNA covering the polymorphic *HGF* −1652 SNP was evaluated by EMSA, using a LightShift Chemiluminescent EMSA kit (Pierce), according to the manufacturer's directions (20). We used duplex DNA probes composed of complementary oligonucleotides labeled with biotin at the 3′ end: 5′-GATCC/TCTCAAAAGGAATTCT-3′ and 5′-CTAGG/AGAGTTTTCCTTAAGA-3′, with either C/G or T/A at position −1652 (underlined). Nuclear extracts were prepared from primary skin fibroblast cultures, which were derived from the backs of 2 healthy control subjects. The extracts were incubated with biotin-labeled DNA and separated on 4% native polyacrylamide gels. The protein-DNA complex was detected by measuring a chemiluminescent signal. Competition assays were performed using a 400-fold excess of unlabeled duplex DNA as a competitor.

Measurement of serum HGF concentrations. Levels of HGF in serum samples were measured using specific enzyme-linked immunosorbent assay kits (Quantikine; R&D Systems) according to the manufacturer's instructions.

Statistical analysis. The genotype frequency distribution was assessed for Hardy-Weinberg equilibrium. Phenotype frequencies were tested for statistical significance using Pearson's chi-square test for a 2 × 3 contingency table. Corrected P (P_{corr}) values were obtained by multiplying by the number of alleles. Significant differences (overall $P_{corr} < 0.05$) were further analyzed by pairwise comparisons using 2 × 2 chi-square tests. Odds ratios (ORs) with 95% confidence intervals (95% CIs) were calculated for statistically significant differences. Continuous variables are reported as the mean ± SD; they were compared using the Mann-Whitney U test. The correlation coefficient (r) was determined using a single regression model. Cumulative survival rates were calculated using the Kaplan-Meier method, and differences between 2 groups were analyzed by the log rank test. All statistical analyses were performed with SPSS statistical software for Windows version 15.0J.

RESULTS

Clinical characteristics of the SSc patients. Demographic and clinical features of the SSc patients who were enrolled in the present study are summarized in Table 2. There were statistically significant differences in the age at onset of SSc, the disease duration, and the proportions of patients with dcSSc and with anti-U1

Table 2. Demographic and clinical characteristics of the 2 cohorts of SSc patients enrolled in the study*

Feature	SSc cohort 1, Keio University (n = 159)	SSc cohort 2, Tokyo Women's Medical University (n = 155)
% female	85	91
Age at onset of SSc, mean ± SD years	46.9 ± 13.7	42.8 ± 12.1†
Disease duration, mean ± SD months	185 ± 111	116 ± 59‡
Clinical features of SSc, % of patients		
Diffuse cutaneous SSc	41	64§
Digital ulcer	30	25
Esophageal involvement	65	53
Heart involvement	7	5
Kidney involvement	3	3
Interstitial lung disease	53	51
Pulmonary arterial hypertension	9	8
End-stage lung disease	11	9
Anti–topo I antibody	37	37
Anticentromere antibody	19	20
Anti–U1 snRNP antibody	18	5¶

* SSc = systemic sclerosis; anti–topo I = anti–topoisomerase I; anti–U1 snRNP = anti–U1 small nuclear RNP.
† $P = 0.005$ versus cohort 1.
‡ $P < 0.0001$ versus cohort 1.
§ $P = 0.0005$ versus cohort 1.
¶ $P = 0.0002$ versus cohort 1.

Table 3. Genotype distribution of single-nucleotide polymorphisms within *HGF* and c-*met* loci in SSc patients with and those without ESLD*

Gene location	Genotype	SSc cohort 1, ESLD		SSc cohort 2, ESLD	
		Present (n = 17)	Absent (n = 126)	Present (n = 13)	Absent (n = 142)
HGF −1652	CC	2 (12)	47 (37)†	3 (23)	53 (37)‡
	CT	8 (47)	69 (55)	5 (38)	77 (54)
	TT	7 (41)	10 (8)§	5 (38)	12 (8)¶
HGF +44222	CC	10 (59)	97 (77)		
	CT	7 (41)	28 (22)		
	TT	0 (0)	1 (1)		
HGF +63555	GG	8 (47)	48 (38)		
	GT	9 (53)	78 (62)		
	TT	0 (0)	0 (0)		
c-*met* −980	TT	15 (88)	98 (78)		
	TA	2 (12)	28 (22)		
	AA	0 (0)	0 (0)		

* In the analysis of systemic sclerosis (SSc) patient cohort 1, a total of 16 patients with a disease duration of <5 years who had not developed end-stage lung disease (ESLD) were excluded. Values are the number (%).
† Overall corrected $P = 0.003$ versus cohort 1 patients with ESLD.
‡ Overall corrected $P = 0.01$ versus cohort 2 patients with ESLD.
§ Pairwise comparison showed a significant difference between patients with and those without the TT genotype ($P = 0.0004$, odds ratio 8.1 [95% confidence interval 2.5–26.0]).
¶ Pairwise comparison showed a significant difference between patients with and those without the TT genotype ($P = 0.004$, odds ratio 6.7 [95% confidence interval 1.9–23.9]).

snRNP antibody between cohorts 1 and 2, but the frequencies of organ involvement were similar in the two cohorts.

***HGF* and c-*met* SNPs in SSc patients.** The genotype distribution of the 3 *HGF* SNPs and the 1 c-*met* SNP in the SSc patients and healthy controls conformed to Hardy-Weinberg equilibrium. There was no difference in the distribution of any of the SNPs between the SSc patients in cohort 1 and the healthy controls (data available upon request from the authors). No significant association was observed when comparing the SNP distribution between healthy controls and patients with dcSSc or lcSSc, nor was there any difference in the *HGF* and c-*met* SNP distributions when the SSc patients were grouped according to the presence or absence of involvement of each organ system or each SSc-related ANA.

Association between *HGF* SNP and outcomes of ILD. We next investigated the potential association of SNPs in the *HGF* and c-*met* loci with long-term outcomes of ILD in SSc patients in cohort 1. In this analysis, 16 patients with disease duration of <5 years who had not developed ESLD were excluded. Of the remaining 143 SSc patients, 17 (12%) developed ESLD during the course of the disease. When SSc patients were categorized according to the presence or absence of ESLD, the genotype distribution of *HGF* −1652 was found to be significantly different between the two groups (overall $P_{corr} = 0.003$) (Table 3). In pairwise comparisons, *HGF* −1652 TT was significantly more frequent in patients who developed ESLD than in those who did not (41% versus 8%; $P = 0.0004$, OR = 8.1 [95% CI 2.5–26.0]). However, the frequency of *HGF* −1652 TT was similar in SSc patients with and those without ILD (12% versus 10%). The disease duration was similar in CC, CT, and TT carriers (mean ± SD 208 ± 104 months, 193 ± 110 months, and 205 ± 102 months, respectively).

To confirm the association between the *HGF* −1652 TT genotype and ESLD in SSc patients, 155 SSc patients from an independent cohort (cohort 2) were used in a replication study. All patients in cohort 2 had disease duration of >5 years, and 13 of them (8%) developed ESLD. The distribution of *HGF* −1652 CC, CT, and TT genotypes in cohort 2 was nearly identical to that in cohort 1 (36%, 53%, and 11%, respectively). The genotype distribution of *HGF* −1652 was, again, significantly different between the patients with ESLD and those without (overall $P_{corr} = 0.01$) (Table 3). In pairwise comparisons, *HGF* −1652 TT was significantly more frequent in patients who developed ESLD than in those who did not (38% versus 8%; $P = 0.004$, OR = 6.7 [95% CI 1.9–23.9]). There was no difference in disease duration between CC, CT, and TT carriers (mean ± SD 111 ± 50, 121 ± 66, and 109 ± 41 months, respectively). When the two cohorts were combined, the OR for

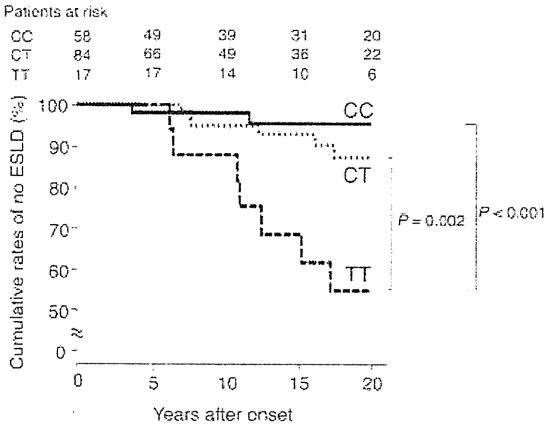

Figure 1. Cumulative rates of survival without end-stage lung disease (ESLD) from the time of systemic sclerosis onset in 159 patients in cohort 1, by *HGF* −1652 genotype. Outcomes were compared using the log rank test. ESLD was defined as the presence of at least 1 of the following 3 features: <50% forced vital capacity, required oxygen supplementation in the absence of pulmonary arterial hypertension, or death due to interstitial lung disease–related causes.

development of ESLD in TT carriers was 7.5 (95% CI 3.2–17.4).

We further evaluated whether the *HGF* −1652 SNP could predict the development of ESLD in the 159 SSc patients in cohort 1. The cumulative rates free of ESLD were compared among the 58 patients with the *HGF* −1652 CC genotype, the 84 with the CT genotype, and the 17 with the TT genotype (Figure 1). The cumulative probability of no ESLD in *HGF* −1652 TT carriers was significantly worse than that in CT or CC carriers ($P = 0.002$ and $P < 0.001$, respectively). There was no significant difference in the cumulative rate between CC carriers and CT carriers.

Influence of the *HGF* −1652 SNP on transcription activity. Since the *HGF* −1652 SNP is located in the promoter region, this SNP may influence transcription activity. To test this hypothesis, we prepared 5 DNA constructs encoding −1756 to −1 (−1652C), −1756 to −1 (−1652T), −1313 to −1, −831 to −1, and −460 to −1, and subjected them to a Dual-Luciferase Reporter Assay system (Figure 2A). The transcription activity of the −1756 to −1 construct carrying the −1652 T allele was significantly lower than the activity of the same region construct carrying the −1652 C allele (mean ± SD 0.16 ± 0.02 versus 0.65 ± 0.03; $P < 0.0001$). The transcription activity of the T allele construct was even lower than the activity of the basic transcriptional activation domain −460 to −1 (0.77 ± 0.05; $P < 0.0001$).

We further assessed interactions between protein and DNA at the *HGF* −1652 polymorphic site, using fibroblast nuclear extracts and EMSA (Figure 2B). Nuclear proteins bound strongly to the T allele probe, but not to the C allele probe. This binding was specific, since an excess amount of the unlabeled probe completely abolished the formation of the complex. This finding indicates that the nuclear factor that bound to the region covering *HGF* −1652 C/T may function as a negative regulator of *HGF* gene transcription.

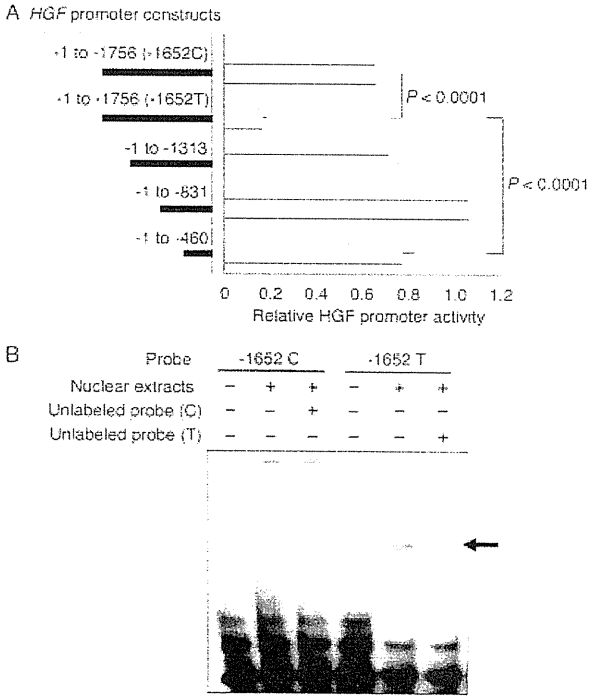

Figure 2. Influence of *HGF* −1652 single-nucleotide polymorphisms (SNPs) on transcription activity. **A,** Transcription activities of reporter constructs harboring *HGF* promoter regions that included nucleotides −460 to −1, −831 to −1, −1313 to −1, −1756 to −1 with a T allele at −1652, and −1756 to −1 with a C allele at −1652. The relative *HGF* promoter activity was calculated as the ratio of firefly luciferase activity to *Renilla* luciferase activity. Values are the mean ± SD of pooled data from 4 observations (duplicate cultures) for each of the 5 constructs. **B,** Electrophoretic mobility shift assay with biotin-labeled probes containing the C and T allele at *HGF* −1652. Unlabeled oligonucleotides were used as competitors to demonstrate binding specificity. **Arrow** indicates the band corresponding to the factor that specifically bound to the *HGF* promoter with a T allele at position −1652. Results are representative of 4 independent experiments using nuclear extracts from primary cultures of skin fibroblasts derived from 2 healthy donors.

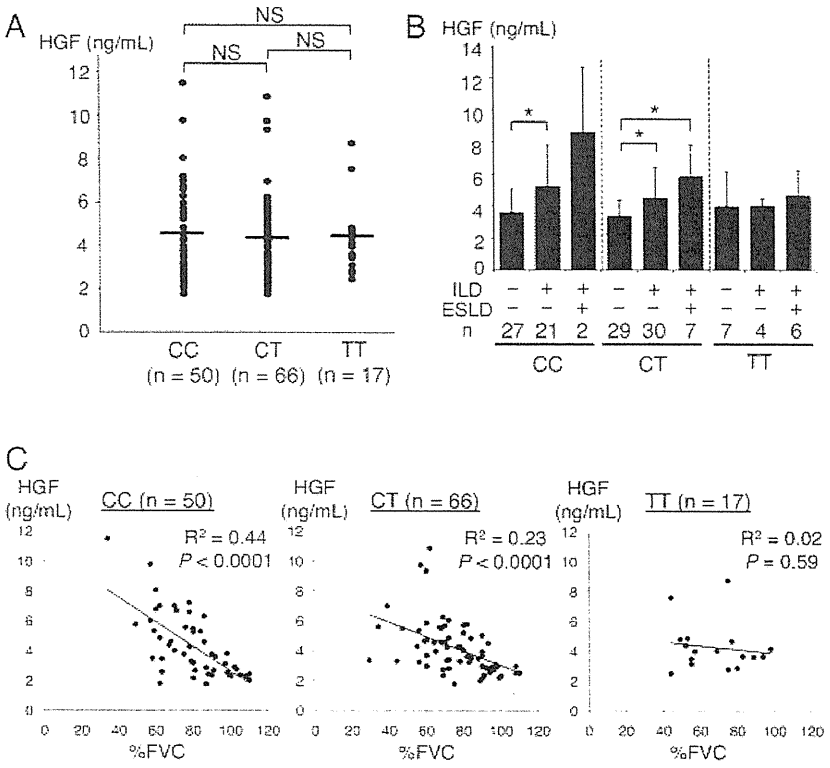

Figure 3. Circulating concentrations of hepatocyte growth factor (HGF) in systemic sclerosis (SSc) patients in cohort 1. **A,** HGF levels in CC, CT, and TT carriers. Each data point represents a single SSc patient; horizontal lines show the mean. NS = not significant ($P > 0.05$). **B,** HGF levels in SSc patients without interstitial lung disease (ILD), those with ILD but without end-stage lung disease (ESLD), and those with ESLD, by carriage of the CC, CT, or TT genotype. * = $P < 0.001$. **C,** Correlation between the serum HGF level and the percentage forced vital capacity (%FVC) in CC, CT, and TT carriers.

Influence of *HGF* −1652 SNP on circulating HGF levels. We measured serum HGF concentrations in 133 SSc patients in cohort 1 and found that there was no difference in the levels between CC, CT, and TT carriers (mean ± SD 4.3 ± 2.1 ng/ml, 4.2 ± 1.8 ng/ml, and 4.2 ± 1.6 ng/ml, respectively) (Figure 3A). We then compared serum HGF levels in the presence or absence of individual organ involvement. ILD was the only organ involvement associated with the HGF level, with a significantly increased level of HGF in patients with ILD than in those without (mean ± SD 4.6 ± 2.0 ng/ml versus 3.8 ± 1.6 ng/ml; $P = 0.008$). We therefore compared the serum HGF levels among patients without ILD, those with ILD and no ESLD, and those with ESLD separately in CC, CT, and TT carriers (Figure 3B). An increased HGF concentration in the presence of ILD or ESLD as compared with the absence of ILD was observed in CC and CT carriers, but not in TT carriers.

We next examined potential correlations between circulating HGF levels and the %FVC in CC, CT, and TT carriers (Figure 3C). A strong negative correlation was observed in CC and CT carriers, suggesting up-regulation of HGF upon progression of ILD. In contrast, TT carriers had a relative inability to increase the level of HGF in the circulation, even in the presence of advanced ILD with low %FVC.

DISCUSSION

In this study, we did not detect any association between the selected SNPs within the *HGF* and c-*met* loci and SSc in the Japanese population. However, our

data, which were obtained from 2 different cohorts of SSc patients, clearly demonstrated that the SNP at *HGF* −1652 was associated with an increased risk of ESLD in SSc patients. Since this SNP did not correlate with the presence or absence of ILD, it may modulate ongoing pathogenic processes in SSc-associated ILD, rather than its susceptibility. Genotyping for *HGF* −1652 SNP in SSc patients may be useful in predicting ILD outcomes and in deciding whether ILD should be actively treated or not.

The functional experiments identified a novel major repressor site in the *HGF* promoter; the presence of a T allele at position −1652 is critical to transcriptional suppression, which would reduce HGF production and impair its antifibrotic effects. SNPs in the promoter region of the gene potentially alter the affinity of DNA–nuclear protein interactions and, in turn, affect transcription efficiency. EMSA findings indicated the presence of a nuclear factor(s) that selectively binds to the *HGF* promoter region, with a T allele at position −1652. Since the T allele displayed lower promoter transcription activity, a nuclear factor(s) bound to the region covering the SNP at *HGF* −1652 might function as a negative transcription regulator.

When potential transcription factors capable of binding to the nucleotide sequence across the polymorphic site were searched using the online prediction site TFBIND (online at http://tfbind.ims.u-tokyo.ac.jp/), several molecules were selected. These included serum response factor, pre-B cell leukemia transcription factor 1, sex-determining region Y, and yin yang 1 (YY-1). Of these, YY-1 is a multifunctional protein that can activate or repress gene expression involved in proliferation, differentiation, and apoptosis, depending on the cell type (21), and is also the factor that preferentially binds to the *HGF* promoter region with a T allele. However, commercially available anti-YY-1 antibodies did not produce a supershift on EMSA (results not shown). Further studies are necessary to identify the nuclear factor(s) that controls the transcription efficiency of the *HGF* gene at this repressor site.

In SSc-associated ILD, extensive extracellular matrix deposits impair the ability of lung epithelial cells to regenerate, resulting in accelerated lung tissue damage and respiratory failure. Numerous studies have shown HGF to be an endogenous antifibrotic factor in the lungs, ameliorating fibrotic lesions and preserving lung function in experimental animal models of pulmonary fibrosis (22–25). HGF exerts its antifibrotic effects on pulmonary function by reducing the production of type I collagen and CTGF, and increasing the production of matrix metalloproteinase 1 in lung fibroblasts (12,26). HGF also assists in regenerating the alveolar structure by promoting alveolar type II cell proliferation (27). Since HGF plays a beneficial role in lung tissue remodeling, the severity and progression of ILD would be influenced by the patient's ability to express this factor.

The association reported here between the functional SNP located on the *HGF* promoter and the SSc patient's risk of developing ESLD may support this theory. In addition, our results suggest that individuals possessing the *HGF* −1652 TT genotype lack the ability to produce HGF in response to ongoing fibrotic processes, such as progression of ILD, and their antifibrotic activity may be impaired by an intrinsically low HGF response. In this regard, data available at the NCBI database (28) show that the *HGF* −1652 TT genotype is more common in African Americans than in Caucasians (32% versus 17%), which may explain why African American SSc patients show a defective HGF response in the circulation and lungs (12) and have more progressive ILD (9–11) as compared to Caucasian patients. Impaired HGF signaling pathways in lung fibroblasts, which have been reported in African American SSc patients (12), also play a role in the ethnic differences in ILD severity.

In summary, our findings suggest that the SNP within the *HGF* promoter region modulates the severity of SSc-associated ILD by controlling *HGF* transcriptional efficiency. The strength of the observed association warrants a larger prospective study of SSc patients of various ethnic backgrounds.

ACKNOWLEDGMENTS

We thank Yuka Okazaki and Mutsuko Ishida for excellent technical support and Yuko Kaneko for assisting with the statistical analysis.

AUTHOR CONTRIBUTIONS

All authors were involved in drafting the article or revising it critically for important intellectual content, and all authors approved the final version to be published. Dr. Kuwana had full access to all of the data in the study and takes responsibility for the integrity of the data and the accuracy of the data analysis.

Study conception and design. Kuwana.

Acquisition of data. Hoshino, Satoh, Kawaguchi.

Analysis and interpretation of data. Hoshino, Satoh, Kawaguchi, Kuwana.

REFERENCES

1. Agarwal SK, Tan FK, Arnett FC. Genetics and genomic studies in scleroderma (systemic sclerosis). Rheum Dis Clin North Am 2008;34:17–40.

2. Varga J, Abraham D. Systemic sclerosis: a prototypic multisystem fibrotic disorder. J Clin Invest 2007;117:557–67.
3. Ueki T, Kaneda Y, Tsutsui H, Nakanishi K, Sawa Y, Morishita R, et al. Hepatocyte growth factor gene therapy of liver cirrhosis in rats. Nat Med 1999;5:226–30.
4. Kawaguchi Y, Harigai M, Hara M, Fukasawa C, Takagi K, Tanaka M, et al. Expression of hepatocyte growth factor and its receptor (c-met) in skin fibroblasts from patients with systemic sclerosis. J Rheumatol 2002;29:1877–83.
5. Mizuno S, Matsumoto K, Li MY, Nakamura T. HGF reduces advancing lung fibrosis in mice: a potential role for MMP-dependent myofibroblast apoptosis. FASEB J 2005;19:580–2.
6. Inoue T, Okada H, Kobayashi T, Watanabe Y, Kanno Y, Kopp JB, et al. Hepatocyte growth factor counteracts transforming growth factor-β1, through attenuation of connective tissue growth factor induction, and prevents renal fibrogenesis in 5/6 nephrectomized mice. FASEB J 2003;17:268–70.
7. Dai C, Liu Y. Hepatocyte growth factor antagonizes the profibrotic action of TGF-β1 in mesangial cells by stabilizing Smad transcriptional corepressor TGIF. J Am Soc Nephrol 2004;15:1402–12.
8. Kawaguchi Y, Harigai M, Fukasawa C, Hara M. Increased levels of hepatocyte growth factor in sera of patients with systemic sclerosis. J Rheumatol 1999;26:1012–3.
9. McNearney TA, Reveille JD, Fischbach M, Friedman AW, Lisa JR, Goel N, et al. Pulmonary involvement in systemic sclerosis: associations with genetic, serologic, sociodemographic, and behavioral factors. Arthritis Rheum 2007;57:318–26.
10. Greidinger EL, Flaherty KT, White B, Rosen A, Wigley FM, Wise RA. African-American race and antibodies to topoisomerase I are associated with increased severity of scleroderma lung disease. Chest 1998;114:801–7.
11. Kuwana M, Kaburaki J, Arnett FC, Howard RF, Medsger TA Jr, Wright TM. Influence of ethnic background on clinical and serologic features in patients with systemic sclerosis and anti–DNA topoisomerase I antibody. Arthritis Rheum 1999;42:465–74.
12. Bogatkevich GS, Ludwicka-Bradley A, Highland KB, Hant F, Nietert PJ, Singleton CB, et al. Impairment of the antifibrotic effect of hepatocyte growth factor in lung fibroblasts from African Americans: possible role in systemic sclerosis. Arthritis Rheum 2007;56:2432–42.
13. Subcommittee for Scleroderma Criteria of the American Rheumatism Association Diagnostic and Therapeutic Criteria Committee. Preliminary criteria for the classification of systemic sclerosis (scleroderma). Arthritis Rheum 1980;23:581–90.
14. Medsger TA Jr. Systemic sclerosis (scleroderma), localized scleroderma, eosinophilic fasciitis and calcinosis. In: Arthritis and allied conditions: a textbook of rheumatology. McCarty DJ, editor. 11th ed. Philadelphia: Lea & Febiger; 1989. p. 1118–65.
15. Kuwana M, Kaburaki J, Okano Y, Tojo T, Homma M. Clinical and prognostic associations based on serum antinuclear antibodies in Japanese patients with systemic sclerosis. Arthritis Rheum 1994;37:75–83.
16. Medsger TA Jr, Silman AJ, Steen VD, Black CM, Akesson A, Bacon PA, et al. A disease severity scale for systemic sclerosis: development and testing. J Rheumatol 1999;26:2159–67.
17. Takiuchi S, Mannami T, Miyata T, Kamide K, Tanaka C, Kokubo Y, et al. Identification of 21 single nucleotide polymorphisms in human hepatocyte growth factor gene and association with blood pressure and carotid atherosclerosis in the Japanese population. Atherosclerosis 2004;173:301–7.
18. Hirakawa M, Tanaka T, Hashimoto Y, Kuroda M, Takagi T, Nakamura Y. JSNP: a database of common gene variations in the Japanese population. Nucleic Acids Res 2002;30:158–62.
19. Miyazawa K, Kitamura A, Kitamura N. Structural organization and the transcription initiation site of the human hepatocyte growth factor gene. Biochemistry 1991;30:9170–6.
20. Schreiber E, Matthias P, Muller MM, Schaffner W. Rapid detection of octamer binding proteins with 'mini-extracts,' prepared from a small number of cells. Nucleic Acids Res 1989;17:6419.
21. He Y, Casaccia-Bonnefil P. The yin and yang of YY1 in the nervous system. J Neurochem 2008;106:1493–502.
22. Dohi M, Hasegawa T, Yamamoto K, Marshall BC. Hepatocyte growth factor attenuates collagen accumulation in a murine model of pulmonary fibrosis. Am J Respir Crit Care Med 2000;162:2302–7.
23. Mizuno S, Matsumoto K, Li MY, Nakamura T. HGF reduces advancing lung fibrosis in mice: a potential role for MMP-dependent myofibroblast apoptosis. FASEB J 2005;19:580–2.
24. Watanabe M, Ebina M, Orson FM, Nakamura A, Kubota K, Koinuma D, et al. Hepatocyte growth factor gene transfer to alveolar septa for effective suppression of lung fibrosis. Mol Ther 2005;12:58–67.
25. Gazdhar A, Fachinger P, van Leer C, Pierog J, Gugger M, Friis R, et al. Gene transfer of hepatocyte growth factor by electroporation reduces bleomycin-induced lung fibrosis. Am J Physiol Lung Cell Mol Physiol 2007;292:L529–36.
26. Jinnin M, Inn H, Mimura Y, Asano Y, Yamane K, Tamaki K. Effects of hepatocyte growth factor on the expression of type I collagen and matrix metalloproteinase-1 on normal and scleroderma dermal fibroblasts. J Invest Dermatol 2005;124:324–30.
27. Mason RJ, Leslie CC, McCormick-Shannon K, Deterding RR, Nakamura T, Rubin JS, et al. Hepatocyte growth factor is a growth factor for rat alveolar type II cells. Am J Respir Cell Mol Biol 1994;11:561–7.
28. Sherry ST, Ward MH, Kholodov M, Baker J, Phan L, Smigielski EM, et al. dbSNP: the NCBI database of genetic variation. Nucleic Acids Res 2001;29:308–11.

Journal of Neuroimmunology 237 (2011) 87–92

Contents lists available at ScienceDirect

Journal of Neuroimmunology

journal homepage: www.elsevier.com/locate/jneuroim

Autoimmunity to endoplasmic reticulum chaperone GRP94 in myasthenia gravis

Shigeaki Suzuki [a,*], Kimiaki Utsugisawa [b], Kazuo Iwasa [c], Takashi Satoh [d], Yuriko Nagane [b], Hiroaki Yoshikawa [e], Masataka Kuwana [d], Norihiro Suzuki [a]

[a] Department of Neurology, Keio University School of Medicine, Tokyo, Japan
[b] Department of Neurology, Hanamaki General Hospital, Iwate, Japan
[c] Department of Neurology, Kanazawa University Graduate School of Medicine, Kanazawa, Japan
[d] Division of Rheumatology, Department of Internal Medicine, Keio University School of Medicine, Tokyo, Japan
[e] Health Service Center, Kanazawa University Graduate School of Medicine, Kanazawa, Japan

ARTICLE INFO

Article history:
Received 30 March 2011
Received in revised form 2 June 2011
Accepted 20 June 2011

Keywords:
Autoantibody
Autoimmune diseases
ER stress
GRP94
Immunoprecipitation
Myasthenia gravis

ABSTRACT

Immune responses to ER stress have been closely related to the pathogenesis of autoimmune diseases. Using an immunoprecipitation assay, 24 (7.1%) of 336 MG serum samples immunoprecipitated a 90-kDa protein from the muscle cellular extracts, but none of the disease or healthy control sera. The 90-kDa protein was affinity-purified and found to match to ER chaperon GRP94 by matrix-assisted laser desorption/ionization-time of flight mass spectroscopy analysis. The frequency of associated autoimmune diseases was much higher in the anti-GRP94-positive than the -negative patients (71% versus 11%, $p<0.001$). Autoimmunity to ER chaperone GRP94 is associated with a subset of MG patients who have additional autoimmune diseases.

1. Introduction

Myasthenia gravis (MG) is an organ-specific autoimmune disorder characterized by dysfunctional neuromuscular junctions targeted by pathogenic autoantibodies to acetylcholine receptor (AChR) or muscle-specific receptor tyrosine kinase (MuSK) (Meriggioli and Sanders, 2009). A wide range of clinical presentations and associated features allow classification of MG into several subtypes based on disease distribution, age at onset, thymic abnormality and autoantibodies profiles. Additional autoimmune diseases, observed in 2.3% to 24.2% (mean 12.9%) of MG patients, are also heterogeneous (Kuks and Oosterhuis, 2003). Varied autoimmune diseases including neurological, hematological, and cutaneous disorders are also seen in thymoma-associated MG (Evoli et al., 2007). However, there are no clinical markers predicting the development of additional autoimmune diseases in MG patients.

Many endogenous sources of cellular stress arise in the endoplasmic reticulum (ER) following the accumulation of misfolded proteins, a phenomenon known as ER stress (Zhang and Kaufman, 2006). The ER has evolved a highly specific signaling pathway called the unfolded protein response (UPR) to cope with the accumulation of misfolded proteins. The products of the UPR are known as ER chaperones, such as BIP (H chain binding protein) and GRP94 (glucose-regulated protein 94). Neurodegenerative diseases, such as Alzheimer disease and Parkinson disease, are associated with dysfunction of the UPR (Zhang and Kaufman, 2006). There is also growing evidence that immune response can be adversely affected by abnormalities in the URP, which could potentially contribute to the development of autoimmunity (Todd et al., 2008).

In the present study, we identified a novel autoantibody to GRP94 in the sera of patients with MG using an immunoprecipitation assay with radiolabeled RD (rhabdomyosarcoma cell line) cellular extracts (Suzuki et al., 2005). We investigated the correlation between autoantibodies to GRP94 and clinical features in MG patients.

2. Material and methods

2.1. Patients and clinical samples

We studied clinical samples from 341 patients with MG. The diagnosis of MG was based on clinical, electrophysiologic, and immunologic criteria (Meriggioli and Sanders, 2009). Sera were obtained from 336 patients (118 men and 218 women) who were followed at Keio University Hospital and Hanamaki General Hospital. The mean age at MG onset was

* Corresponding author at: Department of Neurology, Keio University School of Medicine, 35 Shinanomachi, Shinjuku-ku, Tokyo 160-8582, Japan. Tel.: +81 3 5363 3788; fax: +81 3 3353 1272.
E-mail addresses: sgsuzuki@z3.keio.jp (S. Suzuki), kutsugi@s4.dion.ne.jp (K. Utsugisawa), neuiwasa@med.kanazawa-u.ac.jp (K. Iwasa), takashis@kitasato-u.ac.jp (T. Satoh), yrnagane@yahoo.co.jp (Y. Nagane), hiroaki@kenroku.kanazawa-u.ac.jp (H. Yoshikawa), kuwanam@sc.itc.keio.ac.jp (M. Kuwana), nrsuzuki@sc.itc.keio.ac.jp (N. Suzuki).

0165-5728/$ – see front matter © 2011 Elsevier B.V. All rights reserved.
doi:10.1016/j.jneuroim.2011.06.011